Combined Cycle Engine Cascades Achieving High Efficiency

Andy Schroder*[1], Mark Turner†[1], and Rory A. Roberts‡[2]

[1]Department of Aerospace Engineering
University of Cincinnati
Cincinnati, Ohio 45221, U.S.A.
[2] Department of Mechanical and Materials Engineering
Wright State University
Dayton, Ohio 45435, U.S.A.

Abstract

Two combined cycle engine cascade concepts are presented in this paper. The first uses a traditional open loop gas turbine engine (Brayton cycle) with a combustor as the topping cycle and a series of supercritical carbon dioxide ($S-CO_2$) engines as intermediate cycles and a bottoming cycle. A global optimization of the engine design parameters was conducted to maximize the combined efficiency of all of the engines. A combined cycle efficiency of 65.0% is predicted. The second combined cycle configuration utilizes a fuel cell inside of the topping cycle in addition to a combustor. The fuel cell utilizes methane fuel. The waste heat from the fuel cell is used to heat the high pressure air. A combustor is also used to burn the excess fuel not usable by the fuel cell. After being heated, the high pressure, high temperature air expands through a turbine to atmospheric pressure. The low pressure, intermediate temperature exhaust air is then used to power a cascade of supercritical carbon dioxide engines. A combined efficiency of 73.1% using the fuel lower heating value is predicted with this combined fuel cell and heat engine device. Details of thermodynamics as well as the ($S-CO_2$) engines are given.

Introduction

Efficiently converting chemical and thermal energy into useful electrical and mechanical work is one of the greatest engineering challenges today. A number of solutions exist with different power density, fuel efficiency, fuel cost, and component capital and maintenance costs. Each solution in widespread use today provides a balance of these costs. Coal powered systems use a Rankine cycle and have efficiencies advertised up to 46% [1]. They have a high burner efficiency for an external combustion engine because heat is added over a large temperature range. With water as their working fluid, they must operate at very high pressure ratios in order to have a high average heat addition temperature and a low average heat rejection temperature due to the boiling and condensation, which accept and reject most of the heat at a nearly constant temperature. Peak temperature are presently limited to ∼873 K [600°C] at peak operating pressures of 25-29 MPa for these large systems[2, 3].

Brayton cycle engines typically utilize natural gas, kerosene, or diesel fuels. They have peak temperature limited to ∼1,900 K [1,627°C] at ∼4.5 MPa. Internal combustion results in a high burner efficiency. Efficiencies are advertised up to 44% for a simple cycle [4].

Current combined cycles use a Brayton cycle as a topping cycle and a Steam Rankine cycle as a bottoming cycle. Efficiencies of slightly less than 62% are advertised for the lower heating value of their fuel[5, 6]. Combined cycles allow for utilization of high temperature heat at lower pressures and lower temperature heat at high pressure, balancing material operating conditions and stresses.

Supercritical Carbon Dioxide ($S-CO_2$) Cycle Engines are an emerging technology with efficiencies predicted to be over 49% at 923 K [650°C] peak temperature and 35 MPa peak pressure. High working pressures are required in order to harness beneficial properties at supercritical pressures. Supercritical carbon dioxide power cycles are recuperated power cycles that feature high power densities and narrow temperatures of heat addition. A number of earlier works have explored the high level design and applications of supercritical carbon dioxide power cycles[7, 8]. Echogen Power Systems has been developing demonstration scale engines since 2007[9].

Fuel cells can utilize natural gas as a fuel and produce work in the form of direct current electricity. Fuel cells are different from Brayton, Rankine, and supercritical carbon dioxide cycles in that they are a chemical process rather than a heat engine. Fuel cells can have an efficiency of 52%

*Doctoral Candidate, Corresponding Author, Email: info@AndySchroder.com
†Associate Professor
‡Associate Professor

operating below 1,273 K [1,000°C]. Fuel cells are still an emerging technology. The world's largest fuel cell power plant is currently 59MW, in Hwasung City, South Korea [10, 11]. Platzer et al. presented a combined cycle utilizing hydrogen and pure oxygen as the fuel with a hydrogen fuel cell that produces 74% thermal efficiency[12].

The current work explores the use of a Brayton cycle engine as a topping cycle in combination with a series of supercritical carbon dioxide power cycles as intermediate and bottoming cycle engines. An earlier work of Mohagheghi explored a supercritcal carbon dioxide power cycle as part of a combined cycle, but only with a single bottoming cycle, and the results were presented in terms of power output, rather than non-dimensionalized combined cycle efficiency, providing limited usefulness[13]. Other researchers at SoftInWay have studied combined cycles with supercritical carbon dioxide, but fixed important supercritical carbon dioxide power cycle design parameters such as pressure ratio, operating pressure, and recompression fraction. They were also focused on power output, rather than non-dimensionalized combined cycle efficiency. Their study concentrated on exhaust heat source temperature, rather than a coupling with a topping cycle[14]. The configuration studied in this work is the use of a cascade of supercritical carbon dioxide power cycles in place of a single bottoming cycle which is traditionally proposed to be a steam based Rankine cycle. The application of this configuration is base load electrical power generation. This approach aims to increase the overall combined cycle efficiency, as well as leverage a power cycle with a high power density. A second approach uses a fuel cell in combination with a Brayton cycle engine and supercritical carbon dioxide power cycles in order to achieve even higher combined cycle efficiencies. The use of a fuel cell in combination with a Brayton cycle was inspired by earlier works of Roberts [15, 16], except the combustion process was changed to occur after the fuel cell, rather than before the fuel cell. This change was motivated by a desire for higher efficiency rather than higher power density. Other researchers have studied the use of supercritical carbon dioxide engines in a combined cycle configuration with fuel cells, however, their work replaced the traditional Brayton cycle engine with the supercritical carbon dioxide cycle engine, rather than compliment it[17, 18].

The authors do recognize that the use of multiple engines in a combined cycle cascade (or series) may be a known concept, but are not aware of any detailed studies with supercritical carbon dioxide engines that conducted a cycle design optimization, or the use of a detailed heat exchanger model that is appropriate for heat exchangers with wildly variable and dissimilar specific heats.

Methodology

Cycle Layouts

In this work, two combined cycle power plant configurations are studied. The first is a combined cycle engine that uses a simple brayton cycle as the topping cycle and a series of supercritical carbon dioxide power cycles as intermediate and bottoming cycles. The topping cycle is expected to use methane (natural gas, CH_4) or kerosene/diesel as it's fuel. Waste heat from the topping cycle is used to power the intermediate and bottoming cycles.

The second combined cycle configuration is similar to the first, except the topping cycle is a modified Brayton cycle that includes a solid oxide fuel cell inside the pressurized environment. The fuel cell simultaneously produces heat and direct current (DC) electrical work from methane (natural gas, CH_4) fuel. 80% of the fuel is utilized by the fuel cell and then the remaining 20% is later burned in a combustor. The fuel cell heats the products and reactants up to 1,273 K [1,000°C]. Incorporating the solid oxide fuel cell inside the Brayton cycle allows for high temperature fuel and air to be provided by compression of those fluids. Waste heat produced by the fuel cell's electrochemical inefficiency heats the high pressure fluids even further, recovering energy that would otherwise be unusable in a stand alone fuel cell configuration. The excess fuel that is unusable by the fuel cell is then able to be burned in the Brayton cycle engine's combustor. Waste heat from the topping cycle is used to power the intermediate and bottoming cycles, just as with the combined cycle that does not use a solid oxide fuel cell.

The most general representation for these two topping cycle layouts is presented in Figure 1. In the case of the cycle with no fuel cell, the fuel cell will just be omitted from the engine and fuel added directly to the flame holders in the combustor, or one can think of the fuel cell components being inactive. If no load is applied to the fuel cell's electrical circuit, no electrochemical reactions will occur and the fuel will pass through to the combustor to be burned.

Figure 2 depicts the intermediate and bottoming $S-CO_2$ cycle engines. This configuration is nearly identical to a layout described in detail by Schroder and Turner[7], with the exception of reheat being removed. The layout is a recompression, precompression, recuperated $S-CO_2$ cycle with intercooling and improved regeneration. The reader is strongly encouraged to review the authors' previous work studying that general layout in detail. Its general, quad shaft configuration is not typically explored in such a general form by researchers. This combined cycle effort builds on that generality in search of the optimal, peak efficiency design. A combination of these topping, intermediate, and bottoming cycles is shown in Figure 3. Depending on the configuration, a different number of $S-CO_2$ engines can be used in the cascade.

A high pressure ratio is used to heat the fuel and air up

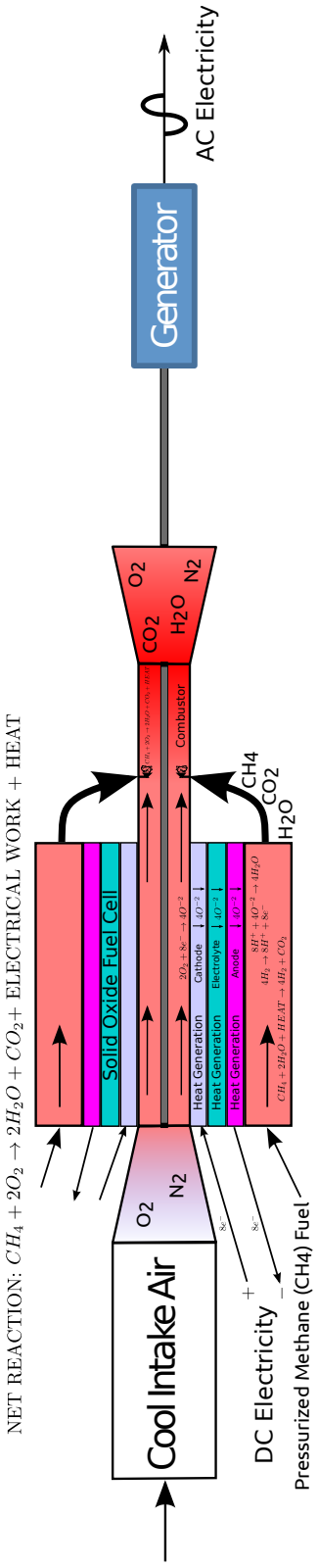

Figure 1: Solid Oxide Fuel Cell integrated into a Brayton Cycle Engine

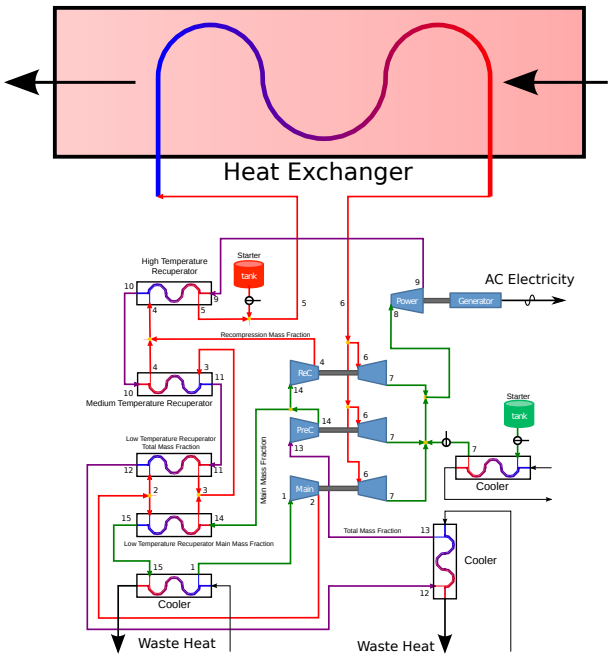

Figure 2: General Supercritical Carbon Dioxide Cycle

to the required inlet temperature of the solid oxide fuel cell rather than a recuperator, which also could have been done. Although use of a recuperator allows for much lower system pressures (could be as low as 0.101MPa), it is believed that such low pressure air to air heat exchangers would be very large and expensive. Additionally, work would not be able to be extracted from the waste heat produced by the fuel cell or from combustion of the unspent fuel. It's possible that a recuperator in combination with a moderate pressure ratio could provide a more balanced configuration and a higher efficiency because the temperature of the waste heat being provided to the supercritical carbon dioxide power cycles would be higher. This configuration of the topping cycle was not presently explored due to the increased modeling complexity and uncertainty on the costs and performance of the air to air heat exchangers.

Although the development of fuel cell technologies has been ongoing for decades, solutions have not yet received widespread market penetration due to the lower technical maturity and higher capital costs compared to competing equipment. Their use is growing however. The configuration presented in this work anticipates some increased maturity of such devices in order for the entire system to be practical.

The solid oxide fuel cell has a temperature inlet requirement of 923 K [650°C]. The design actually considers the use of two different types in series which utilize materials more appropriate for their temperature ranges. However, the two are not distinguished in Figure 1. The lower temperature fuel cell uses silver interconnects and the high temperature fuel cell uses platinum interconnects. The outlet temperature of

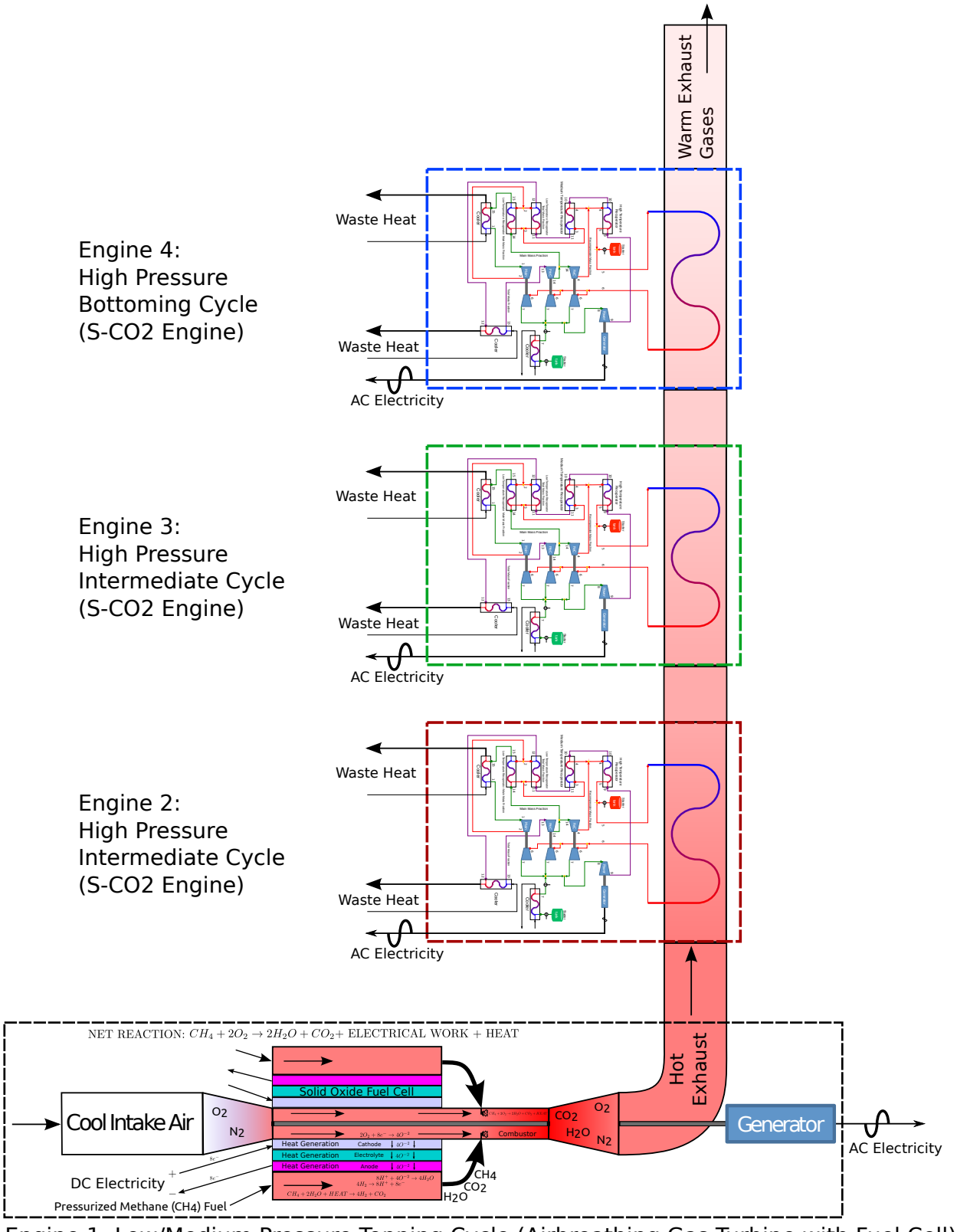

Figure 3: General Combined Cycle Engine Cascade with Solid Oxide Fuel Cell, Brayton Cycle, and Supercritical Carbon Dioxide Cycles

the lower temperature fuel cell and the inlet temperature of the higher temperature fuel cell is 1,093 K [820°C]. The outlet temperature of the higher temperature fuel cell is 1,273 K [1,000°C].

Fuel Cell and Combustion Chemistry

There are a number of processes occurring within the fuel cell. The fuel cell is depicted as part of the gas turbine engine in Figure 1. The methane fuel needs to first be reformed. The reformation process absorbs some waste heat from the fuel cell and some water byproduct and converts CH_4 into hydrogen gas (H_2) and carbon dioxide (CO_2):

$$CH_4 + 2H_2O + HEAT \rightarrow 4H_2 + CO_2 \quad (1)$$

The hydrogen gas then is split into positively charged hydrogen ions (H^+) and electrons that are transferred to the anode:

$$4H_2 \rightarrow 8H^+ + 8e^- \quad (2)$$

The electrons transferred to the anode then flow through the electrical circuit which has a load on it, and then back to the cathode. On the other side of the fuel cell oxygen (O_2) in the supply air is combined with the electrons received on the anode and split into negatively charged oxygen ions (O^{-2}):

$$2O_2 + 8e^- \rightarrow 4O^{-2} \quad (3)$$

The negatively charged oxygen ions then permeate through the cathode, electrolyte, and anode. At the anode, the negatively charged oxygen ions are combined with the positively charged hydrogen ions to form water:

$$8H^+ + 4O^{-2} \rightarrow 4H_2O \quad (4)$$

The net reaction for these processes is a conversion of methane and oxygen into water, carbon dioxide, electrical work, and heat:

$$CH_4 + 2O_2 \rightarrow 2H_2O + CO_2 + ELECTRICAL\,WORK + HEAT \quad (5)$$

Internal to the fuel cell, there is some heat generation in the electrolyte and at the anode and cathode. This heat generation causes the fuel cell's electrochemical efficiency to be lower than ideal. The heat generated is transferred to the fluid which heats up while keeping the fuel cell cool. The heat absorbed in the fuel reformation process is a form of chemical recuperation. The heat absorbed by the water, excess fuel, carbon dioxide, nitrogen, and excess air are pre-heating the air for the brayton cycle.

After the fuel cell, combustion occurs with the remaining methane and excess oxygen. This combustion reaction is similar to that of the fuel cell, without the electrical work output:

$$CH_4 + 2O_2 \rightarrow 2H_2O + CO_2 + HEAT \quad (6)$$

This assumes reactions with nitrogen are not significant to the overall energy balance. The combined reaction of the fuel cell and combustion process is of the same form as the fuel cell by itself presented in Equation (5), except there is some additional heat produced instead of electrical work.

The fuel cell based combined cycle is specified to have 26.3% excess air overall, which is closer to stoichiometric than a traditional gas turbine.

Because the CO_2 is produced in the fuel cell is isolated from the bulk air flow, a potential benefit of a fuel cell is that it may be easier to sequester the CO_2 as part of the process. In order to do so, the reformation process in Equation (1) may need to be a separate step.

Cycle Analysis and Optimization

A variable fluid property cycle analysis code developed by Schroder for studying $S-CO_2$ cycle engines was used as a basis for the analysis [7]. The reader is strongly encouraged to review the authors' previous work as it contains additional details regarding the cycle and heat exchanger modeling that cannot be included here in order to maintain a reasonable document length. Some minor enhancements were made to the variable fluid property cycle analysis code to increase the range of designs the $S-CO_2$ code could explore. The code was improved to incorporate CO_2 to CO_2 heat exchangers which have a non-zero (real) minimum temperature difference between the high and low pressure sides. In the current study, a minimum temperature difference of 5 K was implemented in all of the CO_2 to CO_2 heat exchangers. The previous version of this cycle analysis code was idealized to assume an infinitesimally small minimum temperature difference could exist in the heat exchangers. The cycle analysis code was also modified to eliminate the reheat phase. No reheat is desired in an intermediate or bottoming cycle in a combined cycle power plant because the goal is to extract as much heat from the topping cycle's exhaust gases. The heat transfer from the exhaust gases to the intermediate or bottoming cycle engine is an internal process to the entire system and therefore there is no need to introduce reheat as one may want to do when heat is being added to the system. The maximum pressure was set to 35MPa for the $S-CO_2$ cycles. The minimum system temperature was set to 306 K [33°C]. All other assumptions and component efficiencies utilized for the $S-CO_2$ cycle engines is described by Schroder[7]. Anything related to the $S-CO_2$ engines not specifically stated in this document defaults to that of the earlier $S-CO_2$ cycle study. All of the aforementioned modifications to the earlier work of Schroder and Turner is more clear in the doctoral dissertation of Schroder[19] and the source code made available on Schroder's website[20].

The previous work presented by Schroder demonstrated a brute force technique to explore the design space of the supercritical carbon dioxide power cycle and identify an optimal

design configuration. This exercise proved to be a reliable and straightforward approach as well as distinctly illustrate the highly non-linear nature of the design space. Unfortunately the brute force technique was very time consuming and not practical for exploring systems with a large number of design parameters quickly and at high granularity. As a result, a more intelligent approach was adopted that provided quicker optimization at the expense of uncertainty on achieving a true global optimum. Because the cycle analysis code is based on Python, the available tool sets that were considered was limited to those that can be natively used from within Python. The differential evolution optimizer, part of the SciPy package was used due to it's simple interface, responsive developer, and ability to successfully install and run [21].

The differential evolution optimizer is currently not a parallel optimizer. This results in some limitation in achieving a highly converged optimum solution in a short amount of wall time. After several runs, it was identified that reasonable results could be obtained with the current problem in a reasonable amount of time (∼48 hours).

The differential evolution optimizer is of a class of stochastic population based optimizers. After a solution was found using the differential evolution algorithm, the SciPy ''minimize'' function was used to ''polish'' the results more quickly with a gradient based optimizer. The assumption is that the solution obtained using the differential evolution algorithm is close enough to the global optimum that a gradient based optimizer will not drive the solution away to a local, but non global optimum. A tool was developed that allowed any independent variable in the combined cycle system to be either constrained to a fixed value, optimized, or varied.

In the development of the combined cycle analysis code, many functions were enhanced from Schroder's supercritical carbon dioxide power cycle analysis code. The electrochemical reaction of Equation (5) was implemented for varying equivalence ratios with air. The REFPROP fluid property routines were utilized for air, fuel, and the combustion products [22]. Although very useful for obtaining non-linear fluid properties, REFPROP has many limitations and robustness issues. As a result, combustion products could not be computed below ∼338 K [65°C] because the water vapour began to condense at that temperature and REFPROP could not operate.

REFPROP's methane model had a limited temperature range at 625 K [352°C]. Because of this, the enthalpy of methane at the compressed pressure was extrapolated beyond this limit using ideal gas laws and constant specific heats, in order to calculate the work required to compress the fuel.

The heat exchanger between the exhaust gases and the supercritical carbon dioxide was considerably simpler than the CO_2 to CO_2 heat exchanger model. The CO_2 to exhaust gases heat exchanger assumed negligible pressure drop on the exhaust gas side. It also assumed an infinitesimally small (nearly zero) minimum temperature difference between the CO_2 and exhaust gases. These two assumptions will likely cause a small reduction in overall cycle performance from the current predictions. The current CO_2 to exhaust gas heat exchanger also has been designed such that the average heat capacities of the CO_2 and exhaust gases are nearly equal. Although the specific heat capacities are different between CO_2 and the exhaust gases, the mass flow rate of each CO_2 cycle can be varied such that its average heat capacity (not specific heat capacity) is matched to the exhaust gases. This ability to vary the mass flow rate (and corresponding engine size) of each CO_2 to match the heat capacities of the fluids on both sides of the heat exchanger is believed to be one of the key benefits of the CO_2 compared to a steam based Rankine cycle.

For both combined cycle configurations, a 306 K [33°C] temperature was used at the topping cycle compressor inlet. In the combined cycle configuration without a fuel cell, the compressor pressure ratio was optimized, but limited to 45. For the combined cycle with a fuel cell, the pressure ratio was fixed to 37.15 in order to meet the requirement of a 923 K [650°C] inlet temperature to the fuel cell. A topping cycle compressor efficiency of 84% and turbine efficiency of 90% were used. The combustor in the simple Brayton cycle had a pressure drop of ∼1.5% and peak temperature of 1,890 K [1,617°C]. The hybrid fuel cell Brayton cycle topping cycle does not currently consider any pressure drop in the fuel cell or combustor. The fuel cell was set to have a 58.5% electrochemical efficiency based on the fuel's higher heating value (65% based on the fuel's lower heating value). The fuel cell cycle was configured to have 26.3% excess air and 80% fuel utilization relative to the ideal stoichiometric chemical reactions. It is believed that 85% fuel utilization may be possible; however, a more conservative value of 80% was utilized because of some uncertainty in the performance of the fuel cell under the elevated pressure of 4.35MPa.

Results

Combined Cycle With Simple Gas Turbine

For the combined cycle configuration with a simple Brayton cycle engine with no integrated fuel cell as the topping cycle, a combined cycle efficiency of 65.0% was predicted. Figure 4 shows a combined temperature entropy diagram for all 4 engines in the design that resulted from the optimization process. The color of the lines for each cycle matches the borders around each engine in Figure 3. The topping Brayton cycle engine has a much higher pressure ratio than the $S-CO_2$ cycle engines. Each engine in the cascade has a progressively lower peak temperature than the previous engine in the cascade. Figures 5 through 8 depict temperature entropy diagrams for the 4 different engines in the cascade with appropriate axis ranges for their temperature of operation. The $S-CO_2$ cycle engines' Figures 6 - 8 feature a contour level background emphasizing the high degree of variation in

Engine		Work Fraction	Marginal Combined Cycle Efficiency	Engine Efficiency	Engine Exergy Efficiency
Type	Number	%	%	%	%
Gas Turbine	1	70.05	45.49	45.49	54.28
$S-CO_2$ Engine	2	18.60	12.08	49.59	75.02
$S-CO_2$ Engine	3	9.45	6.14	33.53	63.79
$S-CO_2$ Engine	4	1.90	1.23	14.14	46.10
Combined		100.00	64.95	64.95	77.5

Table 1: Work Split and Efficiencies: Combined Cycle

Engine		Exhaust Gas Heat Exchanger		Power Turbine	Main Compressor
Type	Number	Inlet Temperature	Outlet Temperature	Exit Temperature	Exit Temperature
		K [°C]	K [°C]	K [°C]	K [°C]
Gas Turbine	1	-	903 [630]	903 [630]	925 [652]
$S-CO_2$ Engine	2	903 [630]	645 [372]	698 [425]	348 [75]
$S-CO_2$ Engine	3	645 [372]	441 [168]	494 [221]	329 [56]
$S-CO_2$ Engine	4	441 [168]	342 [69]	348 [75]	313 [40]

Table 2: Selected Temperatures: Combined Cycle

specific heat in the operating regime. The different engines in the cascade feature some or all of the components depicted in the most general layout shown in Figure 2. Depending on the flow split mass fractions, temperatures, pressures, and pressure ratios, some of these components may not exist.

Table 1 shows the work distribution, marginal gain in efficiency due to each engine, the individual engine efficiencies, as well as the exergy efficiency of each individual engine and the combined cycle. The exergy efficiency is defined as the ratio of the actual cycle efficiency to that of an ideal Carnot cycle operating within the same minimum and maximum temperatures. The gas turbine topping cycle produces the majority of the work at 70.05% of the total work output of the combined cycle engine. Each engine produces a diminishing amount of work and marginal gain in combined cycle efficiency. As the temperature drops there is a decreased amount of energy available and the efficiency of each individual engine drops as well.

The topping Brayton cycle engine has an exergy efficiency of 54.28%, which is considerably lower than the second and third engine (the first and second $S-CO_2$ engines) at 75.02% and 63.79%. Low exergy efficiency of the Brayton cycle engine can be explained by high back work ratio, which is the ratio of work required in the compressor relative to the work extracted in the turbine. The large amount of work required to drive the compressor results in additional losses because of inefficiencies in the turbine and compressor. Additional causes for the low exergy efficiency are due to the large range of heat rejection and heat addition by the cycle.

The $S-CO_2$ cycle engines feature moderate back work

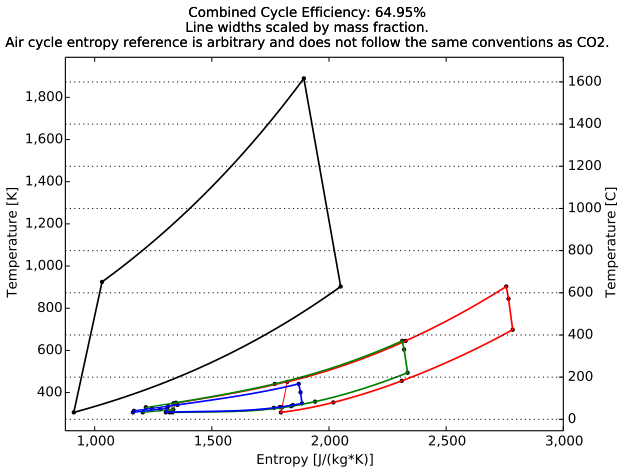

Figure 4: Combined Cycle With Simple Gas Turbine, All Engines: Temperature Entropy Diagram

ratios, locally narrow ranges of heat addition, and narrow ranges of heat rejection, which is what drives their high exergy efficiencies. Unfortunately, there is a limit to how much energy each $S-CO_2$ engine can extract from the exhaust gases so the range of heat addition of the combined cascade of $S-CO_2$ engines is still high. The heat addition of the $S-CO_2$ engines over a large range is an internal process however, so the main penalty on the overall cycle is the large range of heat addition of the topping cycle.

When looking at the high exergy efficiency of the $S-CO_2$

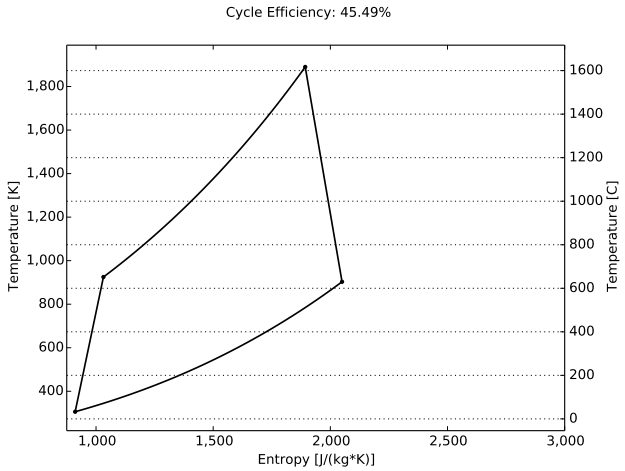

Figure 5: Combined Cycle With Simple Gas Turbine, Engine Number 1: Brayton Cycle, Temperature Entropy Diagram

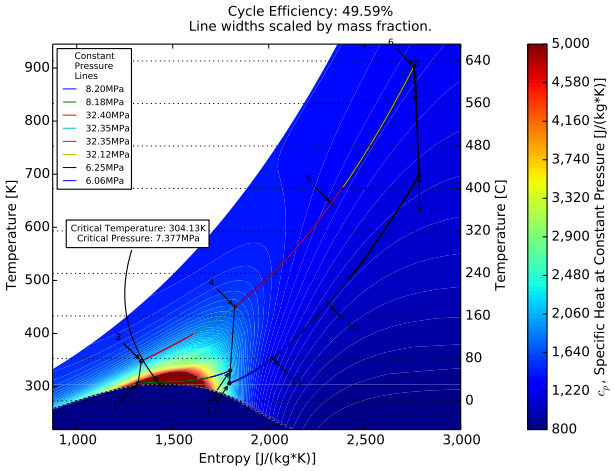

Figure 6: Combined Cycle With Simple Gas Turbine, Engine Number 2: $S - CO_2$ Cycle, Temperature Entropy Diagram with Specific Heat at Constant Pressure Contour Level Background

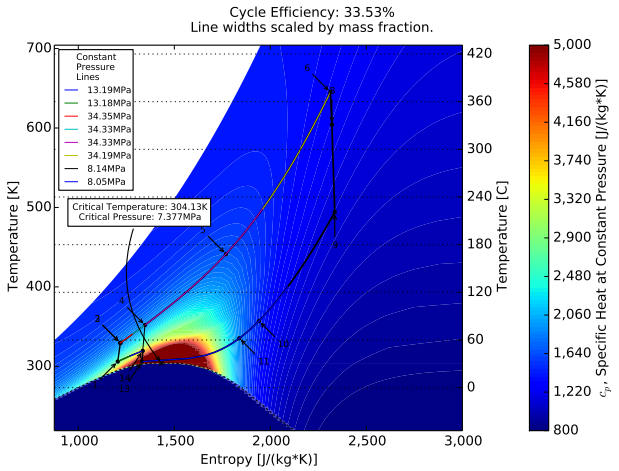

Figure 7: Combined Cycle With Simple Gas Turbine, Engine Number 3: $S - CO_2$ Cycle, Temperature Entropy Diagram with Specific Heat at Constant Pressure Contour Level Background

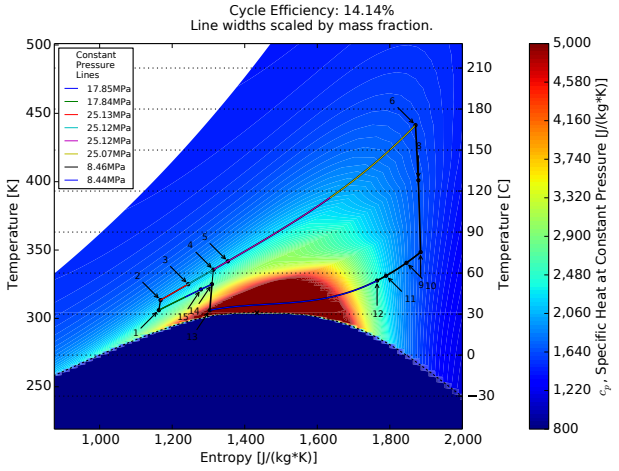

Figure 8: Combined Cycle With Simple Gas Turbine, Engine Number 4: $S - CO_2$ Cycle, Temperature Entropy Diagram with Specific Heat at Constant Pressure Contour Level Background

engines, one may be inspired to replace the topping cycle completely with a $S - CO_2$ engine. There are several reasons doing so is not practical. The first reason is because of the very high working pressures in the $S - CO_2$ engines (up to 35MPa), it is not practical from a strength of materials perspective to operate at higher temperatures than the current configuration. The second reason is that with the $S - CO_2$ engines being closed loop cycles, an external combustion process would require large amounts of regeneration to pre-heat the incoming air in order to maintain a high temperature and narrow temperature range of heat addition. The burner would also have to operate very lean if a narrow temperature range of heat addition were implemented. Recuperators with low pressure, low density air would likely be very large and costly.

The combined cycle exergy efficiency of 77.5% shown in Table 1 is a very high overall exergy efficiency possible through the use of this unique engine cascade that extracts heat from the exhaust gases over limited temperature ranges by different engines. The fourth engine in the cycle features a small overall gain for the system so it's uncertain whether that engine would be economical to include in the system.

Table 2 shows the temperatures at the inlets and outlets of each heat exchanger transferring heat from the exhaust gases

to the $S-CO_2$. Also displayed is the main compressor exit temperatures and the power turbine exit temperatures. The temperature difference between the power turbine and the heat exchanger exit can be significant due to the large specific heat mismatches between the high and low temperature sides of the $S-CO_2$ engine. Because of this larger specific heat mismatch, the high temperature recuperator in the $S-CO_2$ engine is limited because the mass flow rates of the high and low pressure sides have to be equal in the high temperature recuperator.

Although fluid properties were available up to 2,000 K [1,727°C] for nitrogen, water, oxygen, and carbon dioxide, REFPROP could not operate above 1,724 K [1,451°C] with combustion product mixtures because of its inability to work with water vapour in the mixture. A real gas turbine can operate up to ranges of 1,900 K [1,627°C] and higher. Chemically reacting flows were not considered for the combined cycle configuration where no fuel cell was in use. Without a fuel cell, a standard Brayton cycle engine will operate much leaner. As a result, the mass fraction of the fuel during compression is reasonably low and the mass fraction of combustion products is reasonably low. Using pure air is believed to be a reasonable approximation for this engine and allowed for operating up to 1,890 K [1,617°C] without significant issues. When comparing results from pure air based analysis, the efficiencies are to be compared to the lower heating value (LHV) efficiencies of an analysis which considers chemically reacting flows.

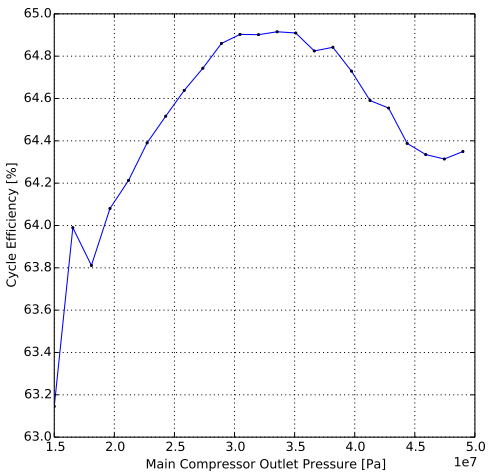

Figure 9: Combined Cycle Efficiency vs $S-CO_2$ Engine Peak Pressure

Some additional studies were conducted to explore the impacts of some design choices on the overall system. In these efforts, a design parameter was varied, from the fixed or optimized values defined previously, to see its impact. Figure 9 shows the combined cycle efficiency vs the $S-CO_2$ engines' peak pressure. This parameter is important because

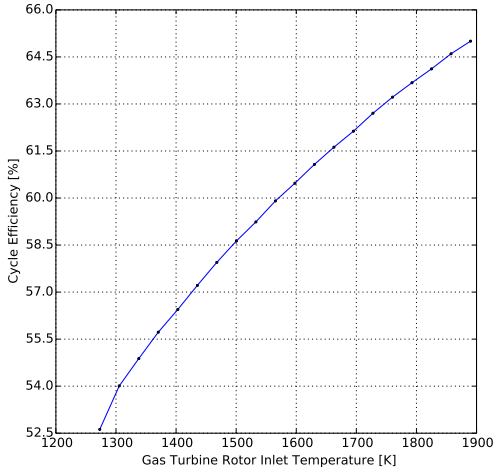

Figure 10: Combined Cycle Efficiency vs Topping Cycle Turbine Inlet Temperature

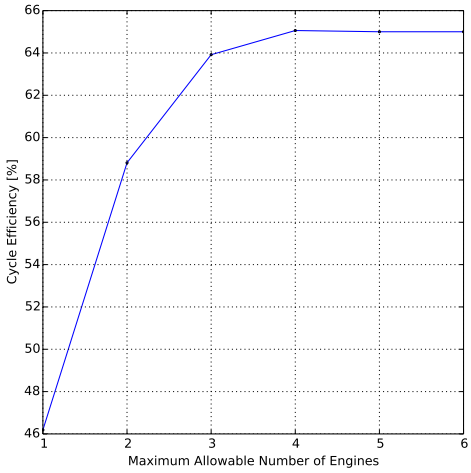

Figure 11: Combined Cycle Efficiency vs Total Number of Engines

the proposed system pressures are typically very high in $S-CO_2$ engines that its useful to know the marginal gain of an increased operating pressure and compare that to the marginal cost, and possibly later constrain an the optimization at a certain peak pressure. It's also interesting to note that an increase in peak pressure does not always result in an increase in efficiency; there is an optimal peak pressure below 49MPa.

Figure 10 shows the overall combined cycle efficiency vs the topping cycle turbine rotor inlet temperature. This parameter is also very important from a cost perspective because higher operating temperatures result in higher initial and maintenance costs. Figure 11 shows the combined cycle efficiency vs the number of engines in the cascade, one engine being a

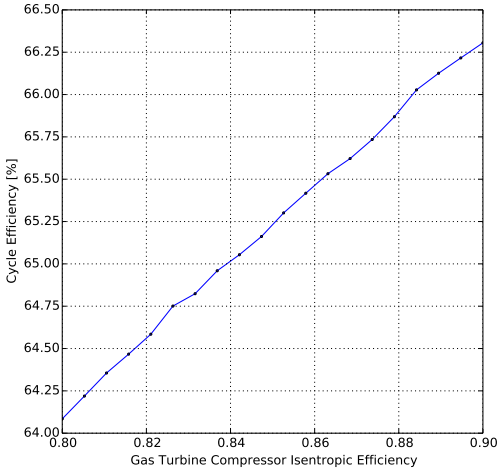

Figure 12: Combined Cycle Efficiency vs Topping Cycle Compressor Isentropic Efficiency

simple gas turbine cycle. In this study, the optimal design was found given the constraint on the maximum allowable number of engines, therefor, the results are different than those presented in Table 1. There is no increase in efficiency with more than four engines and therefore there will not be more than four engines.

Figure 12 shows the overall combined cycle efficiency vs the topping cycle's isentropic efficiency. Because the topping cycle has a much larger pressure ratio and back work ratio, it's important to understand the sensitivity of this component's performance to the overall system because a more efficient component will come at a higher cost. It's important to make note when reviewing all of these parameter sweeps that there appears to be some ''noise'' in the results. This is caused by the optimization process not being an exact one. Each time a new optimization run is conducted, a new random starting population is selected. Reducing the variability between runs can be done by increasing the population size as well as the tolerance on the optimizers convergence. However, doing so will increase the run time and there is a trade off between run time and accuracy and repeatability.

Combined Cycle With Fuel Cell

Using the design optimization process, for the combined cycle configuration with a Brayton cycle engine and integrated fuel cell as the topping cycle, a combined cycle efficiency of 73.09% was predicted using the lower heating value (LHV) of the fuel and 65.84% using the higher heating value (HHV) of the fuel.

Figure 13 depicts the temperature entropy diagrams for all engines in the cascade. Figures 14 through 16 depict temperature entropy diagrams for the 3 different engines in the cascade with appropriate axis ranges for their temperature of operation. Compared to the combined cycle configuration without the integrated fuel cell just presented, there are only two $S - CO_2$ engines compared to three. Shown in Table 3, the topping cycle has a much larger work fraction at 91.15% for the combined fuel cell and gas turbine. The fuel cell has a work fraction of 71.14% and the gas turbine has a work fraction of 20.01%.

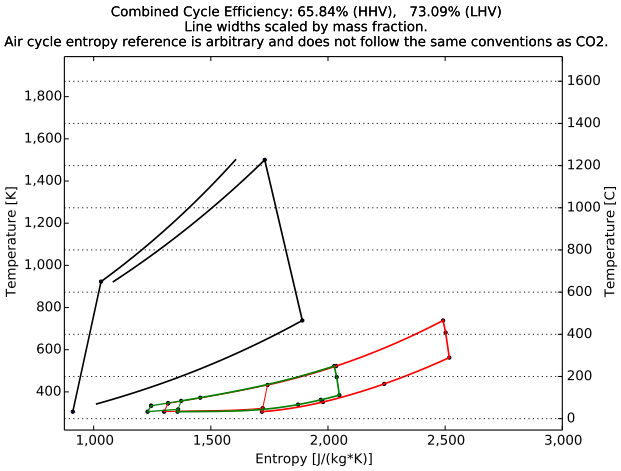

Figure 13: Combined Cycle With Fuel Cell, All Engines: Temperature Entropy Diagram

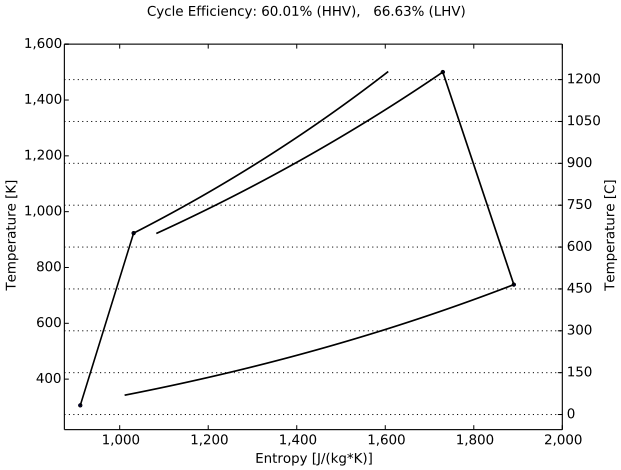

Figure 14: Combined Cycle With Fuel Cell, Engine Number 1: Hybrid Fuel Cell and Brayton Cycle, Temperature Entropy Diagram

Because of these reduced work fractions, the $S - CO_2$ engines contribute much less in improving the overall combined cycle efficiency although they still have fairly high exergy efficiencies. The low work fraction can be explained by observing the inlet temperatures shown in Table 4 for the exhaust gas heat exchangers and comparing them to the combined cycle

Engine		Work Fraction		Marginal Combined Cycle Efficiency				Engine Efficiency		Engine Exergy Efficiency
Type	Number	%		HHV, %		LHV, %		%		%
Fuel Cell	1	71.14	91.15	46.84	60.01	52.00	66.63	52.00 (LHV)	66.63 (LHV)	-
Gas Turbine		20.01		13.17		14.63		30.47 (LHV)		
$S-CO_2$ Engine	2	6.44		4.24		4.71		41.00		69.99
$S-CO_2$ Engine	3	2.41		1.59		1.76		23.02		55.52
Combined		100.00		65.84		73.09%				-

Table 3: Work Split and Efficiencies: Combined Cycle With Fuel Cell

Engine		Exhaust Gas Heat Exchanger		Power Turbine	Main Compressor
Type	Number	Inlet Temperature	Outlet Temperature	Exit Temperature	Exit Temperature
		K [°C]	K [°C]	K [°C]	K [°C]
Fuel Cell + Gas Turbine	1	-	739 [466]	739 [466]	923 [650]
$S-CO_2$ Engine	2	739 [466]	523 [250]	563 [289]	346 [73]
$S-CO_2$ Engine	3	523 [250]	373 [99]	385 [111]	334 [61]

Table 4: Selected Temperatures: Combined Cycle With Fuel Cell

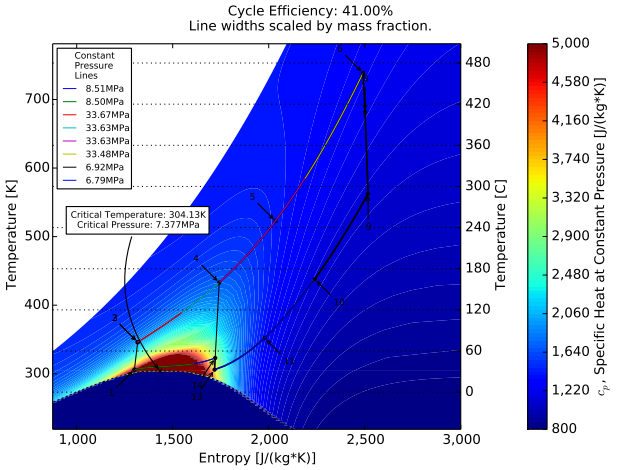

Figure 15: Combined Cycle With Fuel Cell, Engine Number 2: $S-CO_2$ Cycle, Temperature Entropy Diagram with Specific Heat at Constant Pressure Contour Level Background

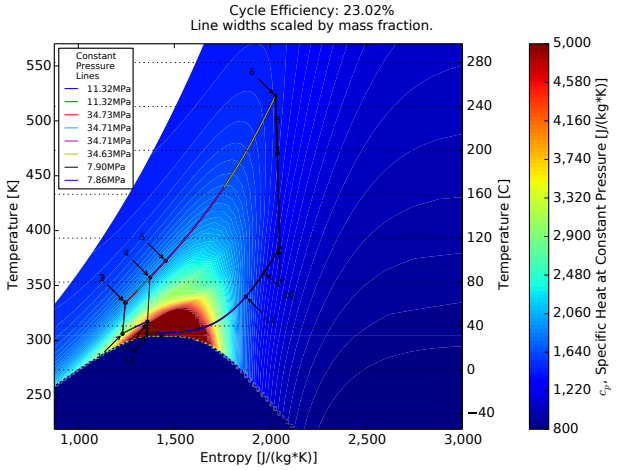

Figure 16: Combined Cycle With Fuel Cell, Engine Number 3: $S-CO_2$ Cycle, Temperature Entropy Diagram with Specific Heat at Constant Pressure Contour Level Background

without a fuel cell shown in Table 2. The highest temperature a $S-CO_2$ engine receives is 739 K [466°C] compared to 903 K [630°C] for the previous combined cycle without a fuel cell.

The fuel cell is naturally a more efficient process than a stand alone Brayton cycle, and the two combined have a LHV efficiency of 66.63%. This is higher than the entire previous combined cycle without a fuel cell! Naturally, there is less waste heat for the $S-CO_2$ to utilize. The combustor also only burns the excess fuel not able to be utilized by the fuel cell, so the peak cycle temperature is 1,500 K [1,227°C], compared to 1,890 K [1,617°C] for the previous combined cycle without a fuel cell. Naturally, the turbine exit temperature will be lower if the turbine inlet temperature is reduced, with a similar pressure ratio. Regardless of the reduced contribution of the $S-CO_2$ cycle engines in this combined cycle configuration, they do still increase the cycle efficiency by over 6 percentage points on a lower heating value basis.

Another important point to note is the itemized fuel cell

efficiency listed in Table 3 may be a little unfairly high relative to the gas turbine. Since the two components are so closely coupled, it's difficult to decide how much of the losses due to fuel and air compression should be attributed to the fuel cell and how much to be attributed to the gas turbine. Presently, all of these losses are attributed to the gas turbine, so the fuel cell gets its fuel and air compressed (and heated) for ''free''. The combined fuel cell and gas turbine efficiencies are not as ambiguous though because they treat the two components as one combined system, sharing the losses. It's also important to point out that the exergy efficiency is not specified in Table 3 for the fuel cell, gas turbine, or the overall combined cycle. The present work has not focused on a detailed exergy flow analysis. A follow on work may be useful to properly identify exergy destruction in each component and more clearly identify the losses that should be attributed to the fuel cell and the gas turbine and to define an overall combined cycle exergy efficiency.

It should be noted that there are some gaps in the lines for the topping air cycle in Figures 13 and 14. The current combined cycle analysis code currently lumps the heat generation of the fuel cell and combustor into a single component that considers the fuel utilization of each. As a result, there is no distinction on the temperature entropy diagram at the fuel cell exit. Also no intermediate species concentrations were computed inside the fuel cell or combustor. As a result, the entropy inside the fuel cell and combustor is not known. A constant pressure line is computed for air from the compressor exit temperature, up to the combustor exit temperature. There is also a constant pressure line computed for combustion products from the compressor exit temperature up to the combustor exit temperature. The actual constant pressure line considering the local species concentration will be somewhere in between these two constant pressure lines. The actual fuel cell and combustor will have some small pressure loss as well, so a constant pressure line is an idealization.

It's important to make some distinction between lower heating value (LHV) and higher heating value (HHV) efficiencies. A LHV efficiency is an efficiency which assumes that the latent heat of vaporization of water in the combustion byproducts is energy that is virtually unobtainable. Thermodynamically, this is not correct. The approach does not conserve energy. Nevertheless, industry has primarily adopted a convention where LHV efficiencies are presented. Using the LHV of a fuel when performing analysis of a Brayton cycle engine for the most part allows for ideal gas analysis to be used with reasonable accuracy because dealing with the non-linearity of the condensation of the water vapour is avoided. Another motivation for the use of LHV efficiencies is because the relative LHV and HHV of different fuels aren't the same. Comparing a HHV efficiency of an engine configuration with a HHV of a similar engine configuration with a different fuel will not result in the same efficiency because they both have different amounts of ''unobtainable'' energy in the water vapour relative to the rest of the energy in the fuel. Using a LHV efficiency and LHV of a fuel allows one to compare engines and fuels without considering the chemical reactions involved.

The temperature at which the water vapour condenses in combustion gases is very low, due to the low partial pressure of the water vapour due to the dominance of nitrogen in air compared to oxygen as well as the very lean operation of most open loop gas turbines. If the water were to completely condense, it would be at such a low temperature that it would not be able to do much useful work. The latent heat of vaporization can still be used for combined heat and power applications though. So, considering a LHV efficiency is not appropriate when an engine can use the latent heat of vaporization of the fuel.

There was some question as to whether there could be any benefit to running the fuel cell at a fuel utilization less than its maximum, combusting more fuel. Similar to the parameter sweeps that were conducted for the combined cycle engine without a fuel cell, a parameter sweep was conducted for the combined cycle engine with a fuel cell, varying the fuel utilization. The results indicated that the combined cycle efficiency increases nearly linearly with fuel utilization and the maximum fuel utilization results in the highest combined cycle efficiency. If the fuel utilization could reach 100%, that would be preferred, but is not a reality due to the way the electrochemical reactions must occur in the fuel cell in an environment with excess fuel present.

Conclusions

The present work demonstrates two different combined cycle configurations that utilize supercritical carbon dioxide power cycles as a means to increase the efficiency by extracting more work from heat in exhaust gases that otherwise would be wasted. One concept uses a traditional open loop gas turbine engine (Brayton cycle) with a combustor as the topping cycle and a series of supercritical carbon dioxide ($S-CO_2$) engines as intermediate cycles and a bottoming cycle. A global optimization of the engine design parameters was conducted to maximize the combined efficiency of all of the engines. A combined cycle efficiency of 65.0% is predicted with three ($S-CO_2$) engines. This assumes dry-cooling.

The other combined cycle configuration concept utilizes a fuel cell inside of the topping cycle in addition to a combustor. The fuel cell utilizes methane fuel. The waste heat from the fuel cell is used to heat the high pressure air. A combustor is also used to burn the excess fuel not usable by the fuel cell. After being heated, the high pressure, high temperature air expands through a turbine to atmospheric pressure. The low pressure, intermediate temperature exhaust air is then used to power a cascade of supercritical carbon dioxide engines. A combined efficiency of 73.1% using the fuel lower heating value is predicted with this combined fuel cell and gas turbine

and two ($S-CO_2$) engines. This is also for a dry-cooling configuration.

The complexity of the layout is high, but each engine in the ($S-CO_2$) engine cascade is a nearly independent module that could be designed, built, and tested independently. Because of the power density of the ($S-CO_2$) engine, its size and weight are much smaller than a comparable steam turbine, in addition to the efficiency benefits.

The general supercritical carbon dioxide engine layout explored is a little studied concept that will require effort to commercialize and mature, but all of the necessary components in the system are believed to be possible to construct. The fuel cell component plays a dominant role in the second combined cycle configuration. Fuel cell technology is still evolving and has not yet reached cost parity with gas turbines. The current cycle layout increases the scale and operating pressure of such devices. It's anticipated that configurations such as the proposed layout could motivate further efforts towards cost reduction in fuel cells due to improved design and manufacturing processes. The studied combined cycle configurations, although complex, are believed to be very feasible.

Future Work

There may be some benefits of using the latent heat of vaporization of water in the combustion products. Because of the higher exergy efficiency of the supercritical carbon dioxide power cycles, there still may be some beneficial work that can be extracted from the condensation of the water, even though the thermal efficiency may be low. It's possible an increase of $\sim$0.5 percentage points of cycle efficiency could be obtained by extracting heat from this condensing water. In order to investigate these possibilities, more exhaustive and realistic exploration can be conducted by increasing the range of operation of the code with combustion products to higher and lower temperatures.

The present analysis considered a cascade of engines where each engine extracted some heat from the topping cycles exhaust gases over a limited range. This approach allows for simpler modeling, design, testing, and controls. An alternate approach could be used where the first supercritical carbon dioxide cycle (the second engine in the cascade) extracts all of the heat down to it's compressor exit temperature. It's waste heat then would be exchanged to the next engine in the cascade, all the way down to that engine's compressor exit temperature. This approach would be more complex to model, test, and control, but it may be simpler from a plumbing perspective and allow for some lower cost components because the temperature difference in the heat exchangers may be higher because the exhaust gases are utilized all the way down to ambient temperature, including the condensation of the water vapour.

The present work focused on steady, on-design analysis. The strengths and weaknesses of the studied configurations in transient and part load conditions have not been considered. It's anticipated that the benefits of each different component in this combined cycle could be harnessed during different load conditions to provide a more stable operation than may be achievable with a simpler combined cycle configuration. Further work should be conducted to explore these design conditions.

The $S-CO_2$ engine cycle analysis code used as a basis for this work does not currently have the capability to model engines which operate below the critical temperature of carbon dioxide. Implementing such capability could identify designs with higher efficiency due to the condensation of carbon dioxide that would occur. This assumption means that all the simulations conducted have dry-cooling which can have huge advantages in many applications. If wet-cooling was available, the carbon dioxide would condense, and an even more efficient cycle would likely result.

References

[1] Alstom/GE. Pulverised coal steam power plant. http://alstomenergy.gepower.com/products-services/product-catalogue/power-generation/coal-and-oil-power/coal-and-oil-power-plants/pulverised-coal-steam-power-plant/ Accessed: November 23rd, 2015.

[2] Frank Cziesla, Jurgen Bewerunge, and Andreas Senzel. Siemens - Lunen - State-of-the-Art Ultra Supercritical Steam Power Plant Under Construction. POWER-GEN Europe 2009, May 2009.

[3] Johna Marion, Frank Kluger, Michael Sell, and Adrian Skea. Advanced Ultra-Supercritical Steam Power Plants. POWER-GEN Asia 2014, September 2014.

[4] GE Power & Water. Marketing Document, LMS100 gas turbine. https://powergen.gepower.com/content/dam/gepower-pgdp/global/en_US/documents/product/lms100-60hz-fact-sheet.pdf Accessed: November 23rd, 2015.

[5] GE Power & Water. Marketing Document, 7HA.01/.02 GAS TURBINE. https://powergen.gepower.com/content/dam/gepower-pgdp/global/en_US/documents/product/gas%20turbines/Fact%20Sheet/7ha-fact-sheet-oct15.pdf Accessed: November 23rd, 2015.

[6] Siemens Energy Sector. Siemens pushes world record in efficiency to over 60 percent while achieving maximum operating flexibility. http://www.siemens.com/press/en/pressrelease/?press=/en/pressrelease/2011/fossil_power_generation/efp201105064.htm Accessed: November 23rd, 2015.

[7] Andy Schroder and Mark Turner. Mapping the Design Space of a Recuperated, Recompression, Precompression Supercritical Carbon Dioxide Power Cycle with Intercooling, Improved Regeneration, and Reheat. 4^{th} International Supercritical CO_2 Power Cycles Symposium, September 2014.

[8] V. Dostal. *A Supercritical Carbon Dioxide Cycle for Next Generation Nuclear Reactors*. PhD thesis, Massachusetts Institute of Technology, Dept. of Nuclear Engineering, 2004.

[9] Echogen Power Systems, LLC. Our Story. `http://www.echogen.com/about/our-story/` Accessed: February 22^{nd}, 2014.

[10] FuelCell Energy, Inc. World's Largest Fuel Cell Park Completed in South Korea. `http://globenewswire.com/news-release/2014/02/19/611481/10068981/en/World-s-Largest-Fuel-Cell-Park-Completed-in-South-Korea.html` Accessed: November 23^{rd}, 2015.

[11] Tildy Bayar, Power Engineering International. Fuel cell power scales up. `http://www.powerengineeringint.com/articles/print/volume-22/issue-7/features/fuel-cell-power-scales-up.html` Accessed: November 23^{rd}, 2015.

[12] M. F. Platzer, W. Sanz, and H. Jericha. Renewable Power Via Energy Ship And Graz Cycle. 15^{th} International Symposium on Transport Phenomena and Dynamics of Rotating Machinery, February 2014.

[13] Mahmood Mohagheghi and Jayanta Kapat. Thermodynamic Optimization Of Recuperated S-CO_2 Brayton Cycles For Waste Heat Recovery Applications. 4^{th} International Supercritical CO_2 Power Cycles Symposium, September 2014.

[14] Leonid Moroz, Petr Pagur, Oleksii Rudenko, Maksym Burlaka, and Clement Joly. Evaluation for Scalability of a Combined Cycle Using Gas and Bottoming SCO_2 Turbines. In *ASME 2015 Power Conference collocated with the ASME 2015 9th International Conference on Energy Sustainability, the ASME 2015 13th International Conference on Fuel Cell Science, Engineering and Technology, and the ASME 2015 Nuclear Forum*. American Society of Mechanical Engineers, 2015.

[15] Rory A. Roberts. *A Dynamic Fuel Cell-Gas Turbine Hybrid Simulation Methodology to Establish Control Strategies and an Improved Balance of Plant*. PhD thesis, University Of California, Irvine, 2005.

[16] Rory A. Roberts, Mitch Wolff, Sean Nuzum, and Adam Donovan. Assessment Of The Vehicle Level Impact For A SOFC Integrated With The Power And Thermal Management System Of An Air Vehicle. ASME 2015 Dynamic Systems and Control Conference, October 2014.

[17] Seong Jun Bae, Yoonhan Ahn, Jekyoung Lee, and Jeong Ik Lee. Hybrid System of Supercritical Carbon Dioxide Brayton Cycle and Carbon Dioxide Rankine Cycle Combined Fuel Cell. In *ASME Turbo Expo 2014: Turbine Technical Conference and Exposition*. American Society of Mechanical Engineers, 2014.

[18] D Sanchez, JM Munoz de Escalona, R Chacartegui, A Munoz, and T Sanchez. A comparison between molten carbonate fuel cells based hybrid systems using air and supercritical carbon dioxide brayton cycles with state of the art technology. *Journal of Power Sources*, 196(9):4347--4354, 2011.

[19] Andrew Schroder. *A Study of Power Cycles Using Supercritical Carbon Dioxide as the Working Fluid*. PhD thesis, University of Cincinnati, Dept. of Aerospace Engineering, 2016.

[20] Andy Schroder. Real Fluid Cycle Analysis Code, Source Code. `http://andyschroder.com/CO2Cycle/SourceCode`.

[21] Differential Evolution, SciPy. `http://docs.scipy.org/doc/scipy/reference/generated/scipy.optimize.differential_evolution.html`.

[22] National Institute of Standards and Technology, Standard Reference Data Program. NIST Standard Reference Database 23: Reference Fluid Thermodynamic and Transport Properties-REFPROP.